MGF Approach Based Analysis Of Energy Detection In $\kappa-\mu$ Shadowed Fading Channels And Diversity Receivers

Hussien Al-Hmood
Electrical and Electronics Engineering Department/ Thi-Qar University/ IRAQ
Hussien.Al-Hmood@eng.utq.edu.iq

Abstract

In this paper, the performance of Energy Detection (ED) over $\kappa-\mu$ shadowed fading channel is investigated using the Moment Generating Function (MGF) of the received Signal-to-Noise Ratio (SNR). The $\kappa-\mu$ shadowed is a generic composite fading channel of $\kappa-\mu$ fading and which represents the impact of multipath in line-of-sight (LoS) communication scenario and Nakagami-m distribution. The study is then extended to include Maximal Ratio Combining (MRC), Square Law Combining (SLC), and Square Law Selection (SLS) diversity receivers. The simulation and numerical results for the Complementary Receiver Operating Characteristics (CROC) and average Area under the CROC (CAUC) curves are given for different scenarios and compared with some previous works. These results show an improvement in the overall detection capability of ED is noticed when the diversity receptions are employed. In contrast to previous works which are limited by the values of the fading parameters, the proposed approach is not restricted by any condition.

Keywords: Energy Detection (ED), $\kappa-\mu$ shadowed, Diversity Reception, Complementary Receiver Operating Characteristics (CROC), Area under the CROC (CAUC).

دالة توليد العزم أساس تحليل مكتشف الطاقة في قنوات الاخفات المغطاة $\kappa-\mu$ مع تنويع الاستقبال

المستخلص

في هذا البحث، تم تحليل الأداء لمكتشف الطاقة فوق قناة الاخفات المغطاة $\kappa-\mu$ باستخدام دالة توليد العزم (MGF) لنسبة الاشارة الى الضوضاء (SNR) المستقبلة. قناة $\kappa-\mu$ المغطاة هي قناة اخفات عامة مركبة من قناة الاخفات $\kappa-\mu$ الذي يمثل تأثير الممرات المتعددة في سيناريو الاتصال في ممر خط الرؤية وتوزيع Nakagami-m. لقد تم توسيع الدراسة لتشمل مخططات تنويع الاستقبال كمركب النسبة العالية (MRC) ومركب قانون المربع (SLC) وانتقاء قانون المربع (SLS). النتائج العددية والتقليدية المعطاة، تَضمنت مُنحني مُكمل خصائص تشغيل المُستقبل (CROC) ومخطط مُعَدل المساحة تحت مُنحني مُكمل

خصـائص تشـغيل المُسـتقبل (CAUC) لسـيناريوهات مختلفة وتمت مقارنة ذلك مع بعض الاعمال السـابقة. لقد بينت تلك النتائج حصـــول تحســـن في مُجمل قابلية الاكتشـــاف لمكتشـــف الطاقه عند اســـتعمال مخططات تنويع الاســـتقبال. على النقيض من الاعمال الســـابقة التي تكون محددة بعوامل الاخفات، العمل المقترح غير مُقيد باي شرط.

الكلمات الرئيسـة: إكتشـاف الطاقة، $\kappa - \mu$ المغطاة، تنويع الاسـتقبال، مُكمل خصـائص تشـغيل المُسـتقبل (CROC)، مُعَدل المساحة تحت الـCROC (CAUC).

1. Introduction

Spectrum sensing via Energy detection (ED) has been extensively used to detect an unknown signals in cognitive radio (CR) and ultra-wide band (UWB) systems. This is because it has lowest hardware complexity in comparison with other methods such as the matched filter and the feature detection. Moreover, ED does not require any prior information of the detecting signal and fading channel [1]. As ED is a non-coherent detection device, its principle work based on evaluating the energy of the received signal over a time window. Then, the results is compared with a predefined threshold value to decide whether the unknown signal is present or absent [2].

In the open technical literature, the performance of ED over different fading channels models has been widely studied using the probability distribution function (PDF) of the received instantaneous signal to noise ratio (SNR). In the first analysis of the performance of ED, the analytic expressions for the detection probability (P_d) and false alarm probability (P_f) over a flat band-limited Gaussian noise channel were derived [3]. Then, the P_d and P_f over Nakagami, Rayleigh and Rice fading channels were provided by depending on the results of [4]. After that, many studies for the behavior of ED over different channels and diversity receptions schemes such as maximal ratio combining (MRC), square law combining (SLC) and square law selection (SLS) have been investigated in [1, 2, 5] and the references therein. Since, in sometimes, the receiver operating characteristic (ROC) curve which is a plot of the average P_d against the P_f does not give clear insight to the behavior of the system, the average area under the ROC (AUC) curve is proposed as a single parameter to measure the total detection capability of the ED [6]. The main advantage of the AUC is to compare the detection performance of two schemes of ED at different SNR values. In some cases, the PDF gives complex non-closed form expressions with infinite series for the performance metrics, i.e., average P_d and average AUC. Hence, the moment generating function (MGF) which is the Laplace transform of the received instantaneous SNR has been proposed in [7, 8] as an alternative method to the PDF approach.

Recently, many works have been done to analyze the performance of ED over $\boldsymbol{\kappa-\mu}$ fading channel that is suggested in [9] as a generalized fading distributions to model the line-of-sight (LOS) communications scenario with better matching to the practical measurements in comparison with Nakagami-$\boldsymbol{m}$ and Nakagami-$\boldsymbol{n}$ (Rice). For example, the analytic expressions of the average $\boldsymbol{P_d}$ of ED in $\boldsymbol{\kappa-\mu}$ fading channels with single receiver and independent and non-identically distributed (i.n.d.) SLS and SLC diversity receivers are derived in [2] using the PDF of the SNR. However, the results are expressed in multivariate hypergeometric functions that are not yet available in mathematical software packages such as MATLAB and MATHEMATICA. Both the average probability of detection and AUC for energy detector in non-identical $\boldsymbol{\kappa-\mu}$ fading channels with MRC, SLC, and SLS diversity schemes are investigated in [10, 11] using the derivative of the MGF approach. But the complexity of the calculation becomes high when the number of diversity branches increases. The average AUC over $\boldsymbol{\kappa-\mu}$ fading channels for no diversity scenario is derived by employing the PDF of the received instantaneous SNR [12]. Thus, these expressions are provided in terms of hypergeometric functions such as Lauricella of multi-variable. In [13], different analytic expressions for the average AUC with SLC scheme in identical $\boldsymbol{\kappa-\mu}$ fading channels are presented.

The wireless signal is also affected by the shadowing that cannot be ignored. Hence, many efforts have been devoted to study the impact of the multipath fading and shadowing simultaneously [14-19]. For instance, in [17-19], the behavior of ED over $\boldsymbol{\kappa-\mu}$ shadowed fading which is suggested in [20] as a composite distribution from the $\boldsymbol{\kappa-\mu}$ fading and Nakagami-$\boldsymbol{m}$ distribution that represents the shadowing impact, is analyzed by using the PDF approach. However, the derived results in the aforementioned references are included an infinite series which requires for a convergence acceleration to find the number of terms that achieves a certain figure of accuracy. Moreover, some of these analysis are employed the approximation in order to obtain a closed-form expressions of the performance metrics. In addition, these efforts do not include all the diversity reception schemes that are studied in this paper.

Motivated by there is no work has been achieved to study the behavior of ED over $\kappa-\mu$ shadowed fading using a MGF of the SNR, we fill this gap by providing the analytic expressions for both the average probability of detection and AUC. The MGF approach is utilized in this paper because it does not provide complicated expressions with functions that are not yet implemented in MATLAB and MATHEMATICA software packages. The analysis is then extended to include the MRC, SLC, and SLS diversity reception techniques with independent and identically distributed (i.i.d.) branches. In contrast to previous works which are applicable for specific scenarios that are related to the values of the fading parameters such as Rician [1], Rician shadowed [15, 16] and $\kappa - \mu$ [10-12] fading channels, our proposed approach is not restricted by any condition. However, all the results that are obtained in the technical literature for the performance of the ED can be evaluated by the derived expressions of this work after substituting specific values of the fading parameters.

2. Energy Detection Model

At the receiver side, the received signal, $r(t)$, follows a binary hypothesis: $\mathbb{H}_0$ and $\mathbb{H}_1$ which represent the signal is absent and present, respectively [5].

$$r(t) = \begin{cases} n(t), & \mathbb{H}_0 \\ hs(t) + n(t), & \mathbb{H}_1 \end{cases} \tag{1}$$

where h is the wireless channel gain, $s(t)$ is the transmitted signal and $n(t)$ is the noise signal at the receiver side. This noise which is additive white Gaussian noise (AWGN) is assumed to be a circularly symmetric complex Gaussian random variable with zero mean and one-side for the power spectral density, N_0.

As explained in [3-5], in the energy detector, the received signal is firstly filtered with an ideal band-pass filter with bandwidth W to limit the noise power as well as to normalize the noise variance. The signal is then squared and integrated over T time interval to evaluate the test statistic, S. This test statistic follows a central chi-square distribution with $2u$ (u is the integer time-bandwidth product) degrees of freedom under hypothesis $\mathbb{H}_0$ or a non-central chi-square distribution with $2u$ degrees of freedom under hypothesis $\mathbb{H}_1$. After that, the test statistic is compared with a predefined threshold value, λ. The P_f and P_d can be calculated by $\Pr(S > \lambda|\mathbb{H}_0)$ and $\Pr(S > \lambda|\mathbb{H}_1)$, respectively, as follows [5]:

$$P_f = \frac{\Gamma\left(u, \frac{\lambda}{2}\right)}{\Gamma(u)} \tag{2}$$

$$P_d = \mathcal{Q}_u(\sqrt{2\gamma}, \sqrt{\lambda}) \tag{3}$$

where $\gamma = |h|^2 E_s/N_0$ is the instantaneous SNR, E_s is the transmitted signal energy, $\Gamma(.)$ is the gamma function, $\Gamma(.,.)$ is the upper incomplete gamma function and $Q_u(.,.)$ is the uth order generalized Marcum-Q function.

3. The $\kappa - \mu$ Shadowed Fading

In the $\kappa - \mu$ shadowed fading, the Nakagami-m distribution is used instead of the lognormal distribution to represent the shadowing impact on the received signal because it leads to simple mathematical composite expressions. Thus, there are three parameters in $\kappa - \mu$ shadowed fading which are κ, μ, and m. The former represents the ratio between the total power of the dominant components and the total power of the scattered waves whereas μ and m stand for the number of the multipath clusters and the shadowing severity index, respectively.

The MGF of the received instantaneous SNR over $\kappa - \mu$ shadowed fading model is expressed as follows [20],

$$\mathcal{M}_\gamma(s) = \frac{D}{(c_1 + s)^{\mu - m}(c_2 + s)^m} \tag{4}$$

where $D = \frac{\mu^\mu m^m (1+\kappa)^\mu}{\bar{\gamma}^\mu (\mu\kappa + m)^m}$, $c_1 = \frac{\mu(1+\kappa)}{\bar{\gamma}}$, $c_2 = \frac{m}{\mu\kappa + m} c_1$ and $\bar{\gamma}$ represents the average SNR.

4. Energy Detection with Single Receiver

4.1 Average Probability of Detection

The $\overline{P_d}$ can be calculated by using the MGF of the SNR as follows [1]

$$\overline{P_d} = \frac{e^{-\frac{\lambda}{2}}}{j2\pi} \oint_{\mathcal{R}} \mathcal{M}_\gamma\left(1 - \frac{1}{x}\right) \frac{e^{\frac{\lambda}{2}x}}{x^u(1-x)} dx \tag{5}$$

where $\mathcal{R}$ is a circular contour of radius $r \in [0, 1)$.

Substituting Eq.(4) in Eq.(5), the $\overline{P_d}$ over $\kappa - \mu$ shadowed fading channel can be written as follows

$$\overline{P_d} = \frac{D e^{-\frac{\lambda}{2}}}{j2\pi(1 + c_1)^{\mu - m}(1 + c_2)^m} \oint_{\mathcal{R}} g_1(x)\, dx \tag{6}$$

where $g_1(x) = \frac{e^{\frac{\lambda}{2}x}}{x^{u-\mu}(1-x)\left(x - \frac{1}{1+c_1}\right)^{\mu - m}\left(x - \frac{1}{1+c_2}\right)^m}$.

To evaluate the contour integral in Eq.(6), the Residue theorem in the complex plane can be applied. The residue of general function $g(x)$ with a poles at $x = x_0$ ($\text{Res}(g; z_0)$) in radius $r \in [0, 1)$ is expressed by

$$\text{Res}(g; x_0) = \frac{1}{(a-1)!}\left[\frac{d^{a-1}(g(x)(x-x_0)^a)}{dx^{a-1}}\right]\Bigg|_{x=x_0} \tag{7}$$

The residue values can be exactly computed by MATLAB and MATHEMATICA software packages.

If both μ and m in Eq.(6) are integer numbers, i.e., μ and $m \in \mathbb{Z}^+$, the $\overline{P_d}$ is given in four cases as in Eq.(8). In this equation, $\Phi_0 = \text{Res}(g_1; 0)$, $\Phi_1 = \text{Res}\left(g_1; \frac{1}{1+c_1}\right)$ and $\Phi_2 = \text{Res}\left(g_1; \frac{1}{1+c_2}\right)$ are the residue of the function $g_1(z)$ at $x = 0$, $x = \frac{1}{1+c_1}$ and $x = \frac{1}{1+c_2}$, respectively.

$$\overline{P_d} = \begin{cases} \dfrac{De^{-\frac{\lambda}{2}}}{(1+c_1)^{\mu-m}(1+c_2)^m}[\Phi_0 + \Phi_1 + \Phi_2] & u > \mu, \mu > m \\ \dfrac{De^{-\frac{\lambda}{2}}}{(1+c_1)^{\mu-m}(1+c_2)^m}[\Phi_0 + \Phi_2]: & u > \mu, \mu \le m \\ \dfrac{De^{-\frac{\lambda}{2}}}{(1+c_1)^{\mu-m}(1+c_2)^m}[\Phi_1 + \Phi_2] & u \le \mu, \mu > m \\ \dfrac{De^{-\frac{\lambda}{2}}}{(1+c_1)^{\mu-m}(1+c_2)^m}\Phi_2: & u \le \mu, \mu \le m \end{cases} \tag{8}$$

It is noted that, when $\kappa \to 0$, $m \to \infty$, $\mu = \underline{m}$ and $\mu = 1$ with some mathematical manipulations, Eq.(8) is reduced to Nakagami-m fading [1, Eqs.(16) and (17)] with $\underline{m}$ is the severity fading index and Rayleigh fading [1, Eq.(18)], respectively. Furthermore, Eq.(8) is equivalent to [15, Eq. (17)] when $m \to \infty$ and $\kappa = K$ which represents the Rician shadowed fading and K is the shaping parameter. In addition, Eq.(8) becomes identical to [1, Eq. (21)] when $m \to \infty$ and $\mu = 1$ with $\kappa = K$, i.e., Rician fading. However, Eq.(8) is expressed in closed-form.

4.2 Average Area under the ROC (AUC)

The $\bar{A}$ can be expressed by the MGF as follows [8]

$$\bar{A} = \frac{1}{j2\pi} \oint_{\mathcal{R}} \frac{\mathcal{M}_\gamma\left(1-\frac{1}{x}\right)}{x^u(2-x)^u(1-x)} dx \tag{9}$$

Plugging Eq.(4) into Eq.(9), the $\bar{A}$ over $\kappa-\mu$ shadowed fading channel can be written as

$$\bar{A} = \frac{D}{j2\pi(1+c_1)^{\mu-m}(1+c_2)^m} \oint_{\mathcal{R}} g_2(x)dx \tag{10}$$

where $g_2(x) = \frac{e^{-\frac{\lambda}{2}x}}{(2-x)^u} g_1(x)$.

The residue theorem is used again to calculate the contour integral in Eq.(10). Accordingly, four different cases for the $\bar{A}$ over $\kappa-\mu$ shadowed channel are obtained as in Eq.(11). In equation, $\Psi_0 = \text{Res}(g_2;0)$, $\Psi_1 = \text{Res}\left(g_2;\frac{1}{1+c_1}\right)$ and $\Psi_2 = \text{Res}\left(g_2;\frac{1}{1+c_2}\right)$ are the residue of the function $g_2(x)$ at $x=0$, $x=\frac{1}{1+c_1}$ and $x=\frac{1}{1+c_2}$, respectively.

$$\bar{A} = \begin{cases} \frac{D}{(1+c_1)^{\mu-m}(1+c_2)^m}[\Psi_0+\Psi_1+\Psi_2]: & u>\mu, \mu>m \\ \frac{D}{(1+c_1)^{\mu-m}(1+c_2)^m}[\Psi_0+\Psi_2]: & u>\mu, \mu\le m \\ \frac{D}{(1+c_1)^{\mu-m}(1+c_2)^m}[\Psi_1+\Psi_2]: & u\le\mu, \mu>m \\ \frac{D}{(1+c_1)^{\mu-m}(1+c_2)^m}\Psi_2: & u\le\mu, \mu\le m \end{cases} \tag{11}$$

It is observed that, when $\kappa \to 0$ and $m \to \infty$ with some mathematical operations, Eq.(11) gives [8, Eq.(5)] with $\mu = m$, i.e., Nakagami-m fading.

5. Energy Detection with Diversity Receivers

5.1 Maximal Ratio Combining (MRC)

In MRC reception, each diversity branch is weighted via multiplying it by factor. This factor is relative to the complex fading coefficient of the branch. If we assume the number of the MRC branches is M, the instantaneous SNR at the output of MRC combiner can be written as follows [1]

$$\gamma^{MRC} = \sum_{i=1}^{M} \gamma_i \tag{12}$$

where γ_i is the instantaneous SNR of ith branch.

The MGF of the received SNR of γ^{MRC} , $\mathcal{M}_{\gamma^{MRC}}(s)$, over the MRC is given by [7]

$$\mathcal{M}_{\gamma^{MRC}}(s) = \prod_{i=1}^{M} \mathcal{M}_{\gamma_i}(s) \tag{13}$$

When all the diversity branches are i.i.d, $\gamma_1 = \gamma_2 \ldots = \gamma_L$. Therefore, $\gamma^{MRC} = M\gamma$ and hence, $\mathcal{M}_{\gamma^{MRC}}(s)$ for i.i.d $\kappa - \mu$ shadowed fading channels is expressed by

$$\mathcal{M}_{\gamma^{MRC}}(s) = \left[\mathcal{M}_{\gamma}(s)\right]^M = \frac{D^M}{(c_1 + s)^{L(\mu-m)}(c_2 + s)^{Lm}} \tag{14}$$

The corresponding P_f^{MRC} and P_d^{MRC} over AWGN channel with MRC scheme are given by [5]

$$P_f^{MRC} = \frac{\Gamma\left(u, \frac{\lambda}{2}\right)}{\Gamma(u)} \quad \text{and} \quad P_d^{MRC} = Q_u\left(\sqrt{2\gamma^{MRC}}, \sqrt{\lambda}\right) \tag{15}$$

Comparing Eqs.(14) and (15) with Eqs.(4) and (3), one can see that the $\overline{P_d}$ and the $\bar{A}$ over $\kappa - \mu$ shadowed fading channels for MRC can be easily calculated by Eqs.(8) and (11), respectively after replacing D, μ and m by D^M, $M\mu$ and Mm, respectively.

5.2 Square Law Combining (SLC)

In this diversity reception technique, before the combining, the signal in each branch is squared and integrated. Thus, the instantaneous SNR at the output the combiner is evaluated by [5]

$$\gamma^{SLC} = \sum_{i=1}^{M} \gamma_i \tag{16}$$

The MGF of γ^{SLC} , $\mathcal{M}_{\gamma^{SLC}}(s)$, can be expressed by

$$\mathcal{M}_{\gamma^{SLC}}(s) = \prod_{i=1}^{M} \mathcal{M}_{\gamma_i}(s) \tag{17}$$

Similar to the MRC diversity reception, when all the diversity branches are i.i.d, the $\mathcal{M}_{\gamma^{SLC}}(s)$ can be expressed by Eq.(13).

The corresponding P_f^{SLC} and P_d^{SLC} over AWGN channel with SLC scheme are given by [5]

$$P_f^{SLC} = \frac{\Gamma\left(Mu, \frac{\lambda}{2}\right)}{\Gamma(Mu)} \quad \text{and} \quad P_d^{SLC} = \mathcal{Q}_{Mu}(\sqrt{2\gamma^{SLC}}, \sqrt{\lambda}) \tag{18}$$

Comparing Eqs.(17) and (18) with Eqs.(13) and (15), one can observe that the difference between the MRC and SLC schemes is the time-bandwidth product which is u in MRC and Mu in SLC. Consequently, the $\overline{P_d}$ and the $\bar{A}$ over $\kappa - \mu$ shadowed fading channels with SLC can be computed by replacing u, D, μ and m by Mu D^M, $M\mu$ and Mm, respectively in Eqs.(8) and (11), respectively.

5.3 Square Law Selection (SLS)

The principle work of SLS is based on selecting the branch of highest energy among all branches. The P_f^{SLS} and P_d^{SLS} over AWGN with SLS reception are expressed by [5]

$$P_f^{SLS} = 1 - \left[1 - \frac{\Gamma\left(u, \frac{\lambda}{2}\right)}{\Gamma(u)}\right]^M \quad \text{and} \quad P_d^{SLS} = 1 - \prod_{i=1}^{M} [1 - \mathcal{Q}_u(\sqrt{2\gamma}, \sqrt{\lambda})] \tag{19}$$

The average probability of detection over i.i.d. $\kappa - \mu$ shadowed fading channels with SLS receivers, $\overline{P_d}^{SLS}$, can be evaluated by inserting Eq.(5) into P_d^{SLS} of Eq.(19). Thus, this yields

$$\overline{P_d}^{SLS} = 1 - \left[1 - \frac{De^{-\frac{\lambda}{2}}}{j2\pi(1+c_1)^{\mu-m}(1+c_2)^m} \oint_{\mathcal{R}} g_1(x)\,dx\right]^M \quad (20)$$

6. Simulation and Numerical Results

In this section, the simulation results are compared with the numerical results using MATLAB software package as well as with some previous works in order to verify the validation of the derived expressions. The simulation results are calculated by Monte-Carlo simulation via generating 10^6 random variables for both $\kappa-\mu$ and Nakagami-m fading distributions. These variables are then combined to obtain the effect of the $\kappa-\mu$ shadowed fading channel. On the other hand, the numerical results are evaluated by the derived Eqs. (8) and (11) and other substitutions for the diversity receptions schemes. In all provided figures, the lines represent the numerical results, while the marks on the curves show the simulation.

Fig. (1) illustrates the complementary ROC (CROC) curve ($\overline{P_{md}} = 1-\overline{P_d}$ versus P_f) of ED in $\kappa-\mu$ shadowed fading for $\bar{\gamma} = 7$ dB, $\kappa = 5$, $u = 1$ and different values for μ and m. In this figure, it is noted that when μ or m increases, the detection diversity becomes better and this leads to improve the detection capability of the ED. In other words, the increasing in μ and m result to large number of the multipath clusters and less shadowing impact, respectively, at the receiver side. For example, at $P_f = 0.1$ and $m = 1$ (fixed), the $\overline{P_{md}}$ for $\mu = 3$ is approximately 11.65% less than the corresponding value for $\mu = 1$. Moreover, when $P_f = 0.1$ and $\mu = 1$ (fixed), the $\overline{P_{md}}$ for $m = 3$ is roughly 21.31% lower than the $\overline{P_{md}}$ for $m = 1$. In this figure, the results of this work for specific scenarios are consistent with their counterparts, namely, Rician [1], Rician shadowed [15, 16], and $\kappa-\mu$ [10] fading conditions that can be obtained by utilizing $\mu = 1$, and $m \to \infty$, $\mu = 1$, and $m \to \infty$, respectively. However, the derived expressions in this paper can be employed for any values of fading parameters that are restricted in [1, 10, 15, and 16].

The results of Fig. (1) are confirmed in Fig. (2) that shows the complementary AUC (CAUC) curves $(1-\bar{A})$ against the average SNR over $\kappa-\mu$ shadowed fading. But, the differences between the compared scenarios are clearer than that are provided in Fig.(1). This proves the advantage of employing the AUC curve in the performance analysis of ED. For instance, for the case $\bar{\gamma} = 10$ dB and $m = 1$ (fixed), the CAUC for

$\mu = 3$ is nearly 32.49% less than for $\mu = 1$. Likewise, when $\mu = 1$ (fixed), the CAUC for $m = 3$ is about 39.72% lower than for the case of $m = 1$. The results for the special scenarios of $\kappa - \mu$ shadowed fading that have been done previously are provided in Fig. (2) and the reader can notice their matching with our analysis.

Figs. (3) and (4) explain the curves of the CROC and CAUC versus average SNR, respectively, of ED single receiver, MRC, SLC, and SLS with $M = 2$ and $M = 4$ branches over i.i.d. $\kappa - \mu$ shadowed fading channels and $\bar{\gamma} = 5$ dB (for Fig.(3)), $\kappa = 3$, $\mu = 2$, $m = 4$, and $u = 1$. In addition, the behavior of ED under Rician, Rician shadowed, and $\kappa - \mu$ is also demonstrated in these figures. As expected, the overall detection capability of ED with diversity reception is better than the case of single receiver. This is because the increasing in either the average SNR as in the MRC scheme or the computed energy at the output of the combiner as in the SLC and SLS receivers. Moreover, ED with the MRC diversity reception outperforms ED with the SLC and SLS schemes. This refers to the high average SNR in the MRC scheme in comparison with the SLC and SLS receivers in which the energy are evaluated at each branch before the combining operation. Furthermore, the performance of ED with SLC is better than that includes SLS scheme. The reason is as follows, in the SLS receivers, the branch with highest energy is chosen as the total test statistic while in the SLC, all the diversity branches are participated in computation of the test statistic. To obtain a good insight about the behavior of ED with diversity receptions, some numerical examples are provided as follows. For instance, in Fig. (3), the values of $\overline{P_{md}}$ at $P_f = 0.01$ (fixed) for single receiver, SLS, SLC, and MRC diversity schemes with $M = 2$ are approximately 0.6419, 0.5006, 0.4161, and 0.3156, respectively. One can see from Fig. (3) and Fig. (4) that the performance of ED with MRC in $\kappa - \mu$ fading is better than the $\kappa - \mu$ shadowed, Rician and Rician shadowed conditions. This is because in $\kappa - \mu$ fading, $\mu = 2$ and $m \to \infty$ whereas in $\kappa - \mu$ shadowed, Rician and Rician shadowed, $\mu = 2$ and $m = 4$, $\mu = 1$ and $m \to \infty$, and $\mu = 1$ and $m = 4$, respectively.

Figs. (5) and (6) demonstrate the behavior of ED versus the time-bandwidth product, u, with $M = 1$, MRC, SLC, and SLS with $M = 2$ and $M = 3$ branches with $P_f = 0.1$ (for Fig.(5)), $\bar{\gamma} = 3$ dB, $\kappa = 1$, $\mu = 4$, and $m = 2$. As it is shown in both figures, when u increases, a substantial degradation in both the $\overline{P_d}$ and the $\bar{A}$ is observed. This is because both the $\overline{P_d}$ and the P_f decrease when u increases. But, the $\overline{P_d}$ decreases slower than the P_f, thus causing a reduction in the performance of the ED. The plot of the $\overline{P_d}$ and the $\bar{A}$ against u is not given in the technical literature. Thus, there is no comparison has been provided in Figs. (5) and (6) with previous works.

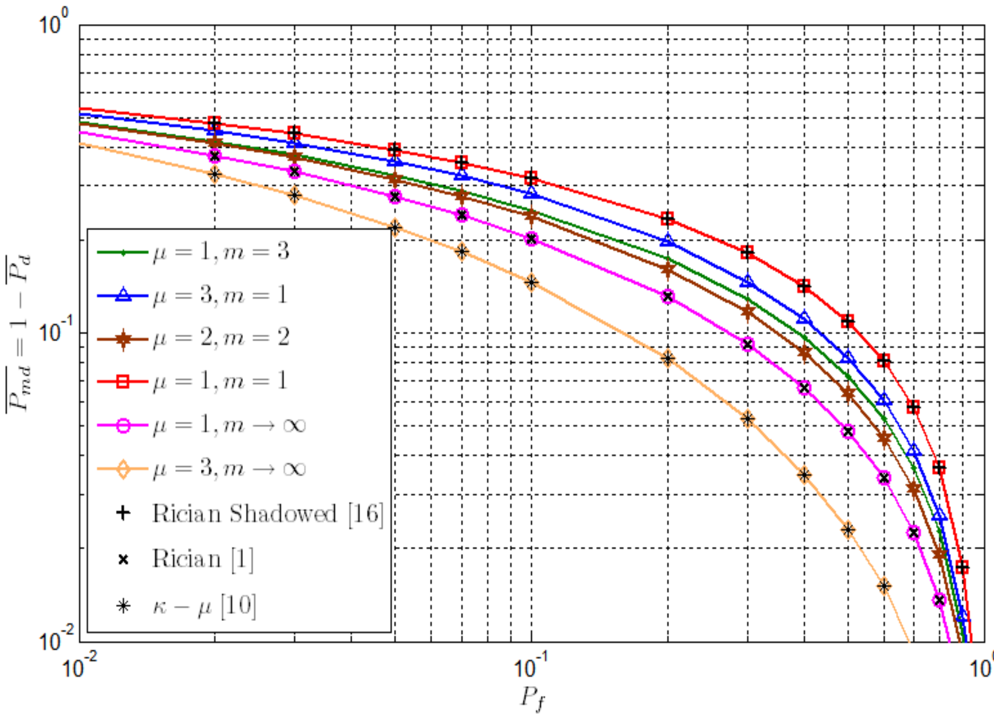

Fig. (1): CROC curves of ED in $\kappa - \mu$ shadowed fading channels for $\bar{\gamma} = 7$ dB, $\kappa = 5$, $u = 1$ and different values for μ and m.

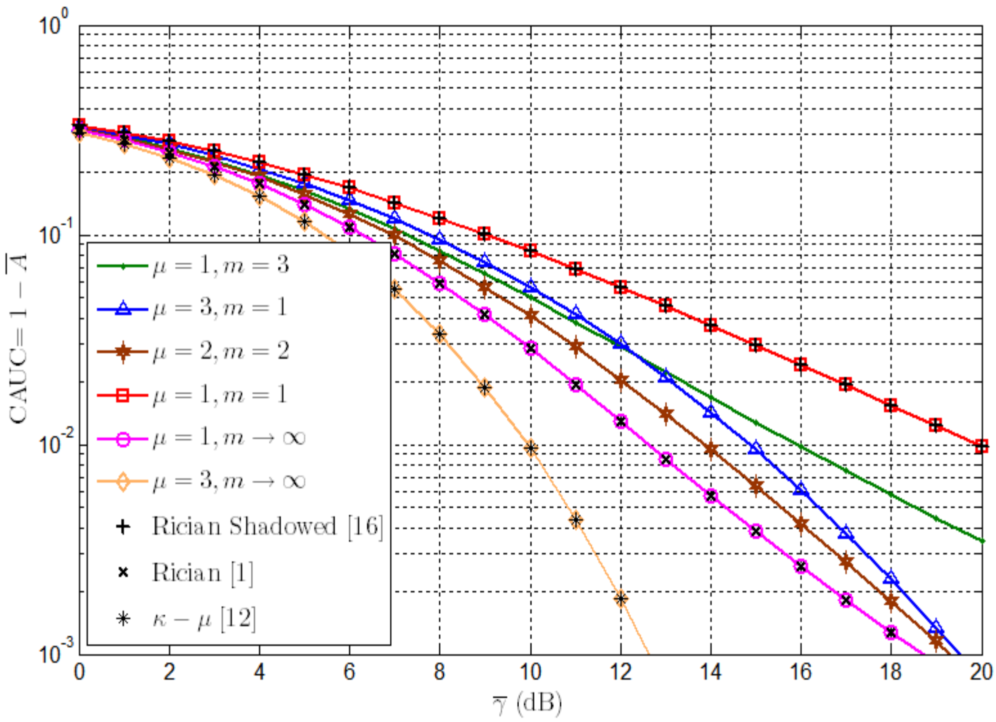

Fig. (2): CAUC of ED against the average SNR, $\bar{\gamma}$, in $\kappa - \mu$ shadowed fading channels for $\kappa = 5$, $u = 1$ and different values for μ and m.

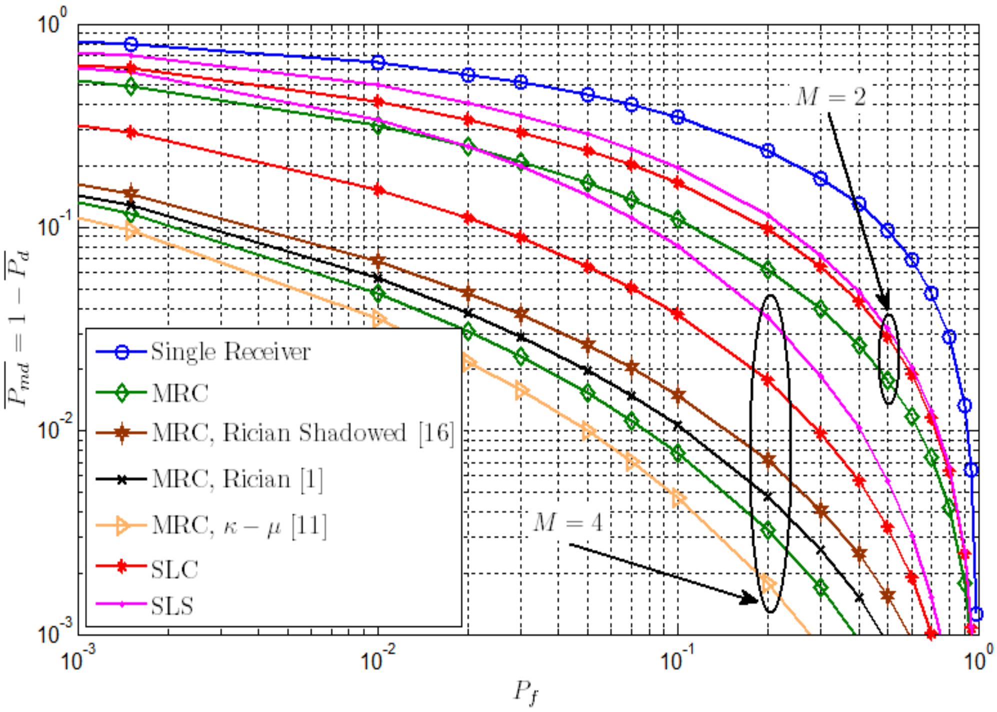

Fig. (3): CROC curves of ED for single receiver, MRC, SLC, and SLS with M = 2 and M = 4 in i.i.d. $\kappa - \mu$ shadowed fading channels and $\overline{\gamma}$ = 5 dB, $\kappa = 3$, $\mu = 2$, $m = 4$, and $u = 1$.

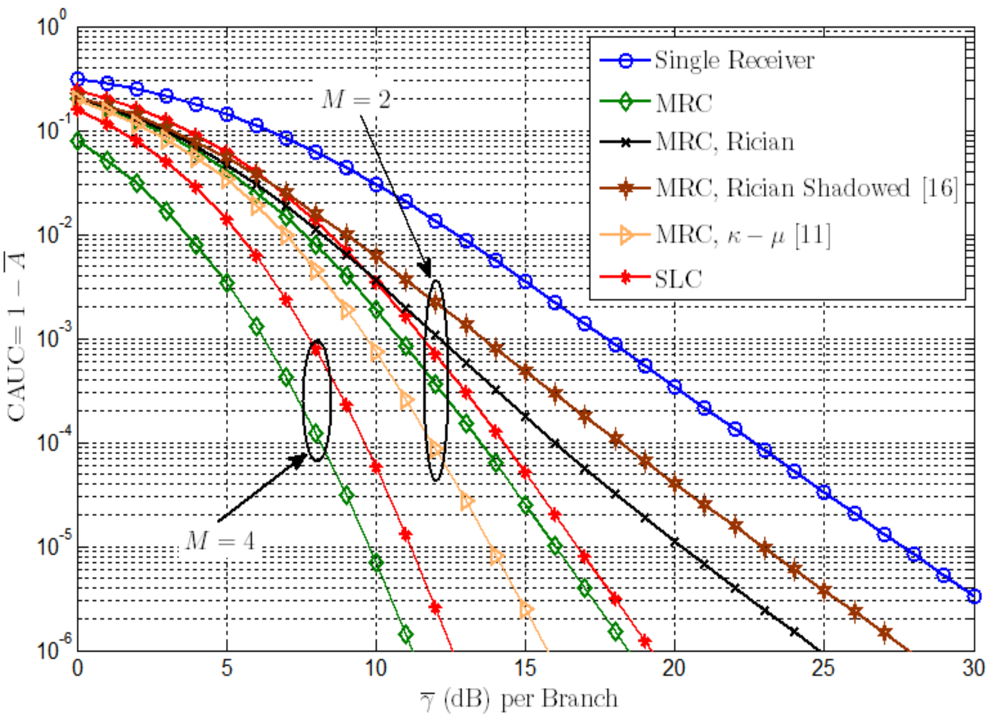

Fig. (4): CAUC curves of ED versus the average SNR, $\overline{\gamma}$, for single receiver, MRC, and SLC with M = 2 and M = 4 in i.i.d. $\kappa - \mu$ shadowed fading channels and $\kappa = 3$, $\mu = 2$, $m = 4$, and $u = 1$.

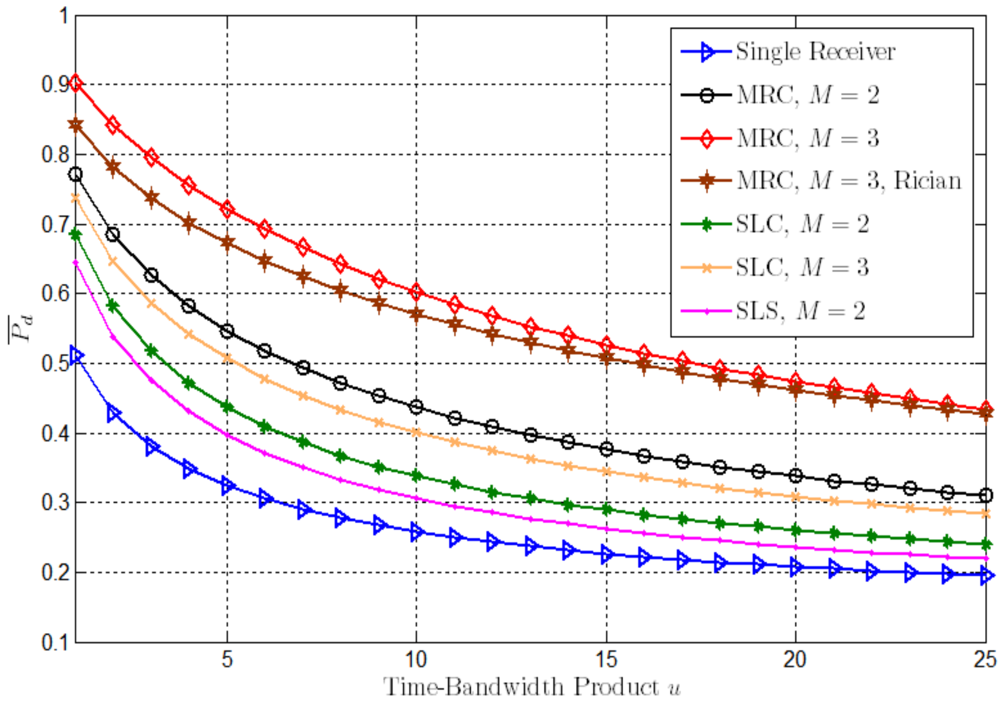

Fig. (5): Average probability of detection, $\overline{P_d}$, of ED versus u for single receiver, MRC, SLC, and SLS with M = 2 and M = 3 in i.i.d. $\kappa-\mu$ shadowed fading channels and $P_f = 0.1$, $\bar{\gamma} = 3$ dB, $\kappa = 1$, $\mu = 4$, and $m = 2$.

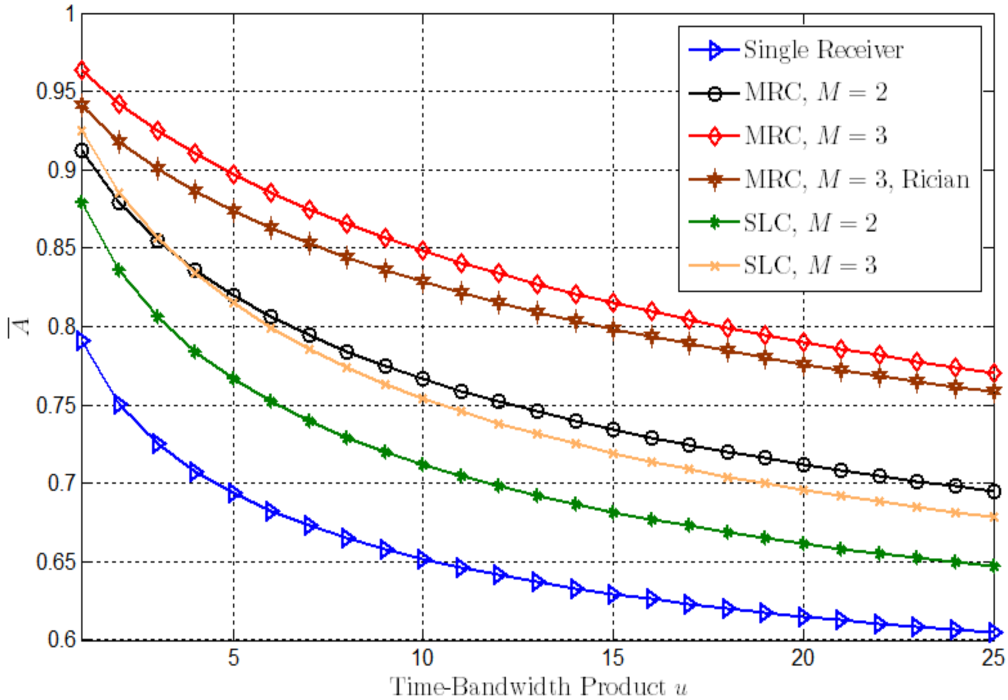

Fig. (6): Average AUC, $\bar{A}$, of ED versus u for single receiver, MRC, and SLC with M = 2 and M = 3 in i.i.d. $\kappa-\mu$ shadowed fading channels and $\bar{\gamma} = 3$ dB, $\kappa = 1$, $\mu = 4$, and $m = 2$.

6. Conclusions

In this paper, we have extensively analyzed the performance of ED over $\kappa-\mu$ shadowed fading channels with no diversity, MRC, SLC and SLS receivers. Both the average P_d and the average AUC were derived in simple exact analytic expressions using the MGF approach. The residue theorem was used to compute the contour integral for the average P_d and the average AUC. From the results, we noted that the detection capability improves when μ or/and m increase. The parameter μ has higher impact on the detectability of ED in comparison with m. Moreover, the ED with MRC has better performance than SLC and SLS. These results can be employed to obtain on good insight about the behavior of ED over different composite fading channels such as Rician shadowed fading with better fitting to the practical measurements than the conventional counterparts.

References

[1] S. P. Herath, N. Rajatheva, and C. Tellambura, "Energy detection of unknown signals in fading and diversity reception," *IEEE Trans. Commun.*, vol. 59, no. 9, pp. 2443–2453, Sep. 2011.

[2] P. Sofotasios, E. Rebeiz, L. Zhang, T. Tsiftsis, D. Cabric, and S. Freear,"Energy detection based spectrum sensing over $\kappa-\mu$ and $\kappa-\mu$ extreme fading channels," *IEEE Trans. Veh. Technol*., vol. 62, no. 3, pp. 1031–1040, March 2013.

[3] H. Urkowitz, "Energy detection of unknown deterministic signals," in *Proc. IEEE*, vol. 55, no. 4, pp. 523–531, Apr. 1967.

[4] V. I. Kostylev, "Energy detection of signal with random amplitude," in *Proc. IEEE ICC*, pp. 1606–1610, May 2002.

[5] F. F. Digham, M. S. Alouini, and M. K. Simon, "On the energy detection of unknown signals over fading channels," *IEEE Trans. Commun.*, vol. 55, no. 1, pp. 21–24, Jan. 2007.

[6] S. Atapattu, C. Tellambura, and H. Jiang, "Analysis of area under the ROC curve of energy detection," *IEEE Trans. Wireless Commun.*, vol. 9, no. 3, pp. 1216–1225, Mar. 2010.

[7] S. Atapattu, C. Tellambura, and H. Jiang, "Energy detection of primary signals over $\eta-\mu$ fading channels," in *Proc.* 4th ICIIS, pp. 118–122, Dec. 2009.

[8] S. Atapattu, C. Tellambura, and H. Jiang, "MGF based analysis of area under the ROC curve in energy detection," *IEEE Commun. Lett.*, vol.15, no.12, pp.1301–1303, Dec. 2011.

[9] M. D. Yacoub, "The $\kappa-\mu$ distribution and the $\eta-\mu$ distribution," *IEEE Antennas Propag. Mag.*, vol. 49, no. 1, pp. 68–81, Feb. 2007.

[10] A. Annamalai, and A. Olaluwe, "On the energy detection of unknown signals in $\kappa-\mu$ and $\eta-\mu$ fading channels with diversity receivers," in *Proc. IEEE Int. Conf. Connected Vehicles and Expo (ICCVE)*, 2013, pp. 127-132.

[11] A. Annamalai, and A. Olaluwe, "Energy detection of unknown deterministic signals in $\kappa-\mu$ and $\eta-\mu$ generalized fading channels with diversity receivers," in *Proc. IEEE* **Int. Conf. Computing Net. and Commun. (ICNC)**, 2014, pp. 761–765.
[12] A. Bagheri, and P. C. Sofotasios, T. A. Tsiftsis, A. Shahzadi, and S. Freear, and M. Valkama, "Area under ROC curve of energy detection over generalized fading channels," in *Proc. IEEE Pers. Ind. and Mob. Rad. Commun. (PIMRC)*, Aug. – Sept. 2015, pp. 656–661.
[13] A. Bagheri, and P. C. Sofotasios, T. A. Tsiftsis, A. Shahzadi, and S. Freear, and M. Valkama, "Spectrum sensing in generalized multipath fading conditions using square-law combining," in *Proc. IEEE* **Int. Conf. Commun. (ICC)**, 2015, pp. 7528-7533.
[14] S. Atapattu, C. Tellambura, and H. Jiang, "Performance of an energy detector over channels with both multipath fading and shadowing," *IEEE Trans. Wireless Commun.*, vol. 9, no. 12, pp. 3662–3670, Dec. 2010.
[15] K. P. Peppas, G. Efthymoglou, V. A. Aalo, M. Alwakeel, and S. Alwakeel, "On the performance analysis of energy detection of unknown signals in Gamma shadowed Rician fading environments," in *Proc. IEEE Pers. Ind. and Mob. Rad. Commun. (PIMRC)*, Sept. 2013, pp. 756–760.
[16] K. P. Peppas, G. Efthymoglou, V. A. Aalo, M. Alwakeel, and S. Alwakeel, "Energy detection of unknown signals in Gamma-shadowed Rician fading environments with diversity reception," *IET Commun.*, vol. 9, no. 2, pp. 196–210, Jan. 2015.
[17] M. S. Aloqlah, "Performance analysis of energy detection-based spectrum sensing in $\kappa-\mu$ shadowed fading,'' *Elect. Lett.*, vol. 50, no. 25, pp. 1944–1946, Dec. 2014.
[18] M. S. Aloqlah, I. E. Atawi, and M. F. Al-Mistarihi, "Further performance results for energy detector operating over $\kappa-\mu$ shadowed fading,'' in *Proc. IEEE Pers. Ind. and Mob. Rad. Commun. (PIMRC)*, Aug. – Sept. 2015, pp. 668–671.
[19] G. Chandrasekaran, and S. Kalyani, "Performance analysis of cooperative spectrum sensing over $\kappa-\mu$ shadowed fading," *IEEE Wireless Commun. Lett.*, vol. 4, no. 5, pp. 553–556, Oct. 2015.
[20] J. Paris, "Statistical characterization of $\kappa-\mu$ shadowed fading,'' *IEEE Trans. Veh. Technol.*, vol. 63, no. 2, pp. 518–526, Aug. 2013.